Optics and Laser Technology 97 (2017) 97–105

Contents lists available at ScienceDirect

Optics and Laser Technology

journal homepage: www.elsevier.com/locate/optlastec

Full length article

Mitigating effect on turbulent scintillation using non-coherent multi-beam overlapped illumination

Lu Zhou [a], Yuzhen Tian [b,*], Rui Wang [b], Tingfeng Wang [b], Tao Sun [b], Canjin Wang [b], Xiaotian Yang [a]

[a] Jilin Provincial Key Laboratory of Architectural Electricity & Comprehensive Energy Saving, School of Electrical Engineering and Computer, Jilin Jianzhu University, Changchun 130118, China

[b] State Key Laboratory of Laser Interaction with Matter, Changchun Institute of Optics, Fine Mechanics and Physics, Chinese Academy of Science, Changchun 130033, China

ARTICLE INFO

Article history:
Received 29 June 2016
Accepted 19 June 2017
Available online 6 July 2017

Keywords:
Atmospheric optics
Atmospheric propagation
Atmospheric turbulence
Adaptive optics
Optical communications

ABSTRACT

In order to find an effective method to mitigate the turbulent scintillation for applications involved laser propagation through atmosphere, we demonstrated one model using non-coherent multi-beam overlapped illumination. Based on lognormal distribution and the statistical moments of overlapped field, the reduction effect on turbulent scintillation of this method was discussed and tested against numerical wave optics simulation and laboratory experiments with phase plates. Our analysis showed that the best mitigating effect, the scintillation index of overlapped field reduced to 1/N of that when using single beam illuminating, could be obtained using this method when the intensity of N emitting beams equaled to each other.

1. Introduction

Laser played an important role in applications such as active imaging, laser communication and ladar [1,2], because of the characteristics of laser, far operation range, small divergence angle and high brightness. However, when laser transmitted long path through atmospheric turbulence, the irradiance fluctuation affected these applications seriously [3–9]. Therefore, if we could reduce the irradiance fluctuation, the performance of these applications could be enhanced.

In this paper, we introduced a simple non-coherent multi-beam illumination model to reduce irradiance fluctuation at the observation plane, under weak turbulence conditions, when the probability distribution function (PDF) of irradiance was modeled as lognormal distribution. This model could be used in active imaging and laser communication system, and was useful for designing optical system and laboratory experiments with phase plates, which the performance is prior to purchasing equipment and conducting experiments. The model of Tellez and Schmidt [10] introduced the theory results of multi-beam model under moderate and strong turbulence, and many others also did some theoretical [5] or experiments [11] research of multi-beam scintillation models under different conditions, but the model developed here just focus on weak turbulence situation for laser active imaging and laser communication, and we treated this model as a simple statistical problem, which did not consider the complexity physical process. The multi-beam scintillation index verified that the non-coherent multi-beam illumination model was useful for mitigating the irradiance fluctuation. Especially when each beam illuminated with equal intensity, the index reduced to 1/N of that of individual beam. In order to test this model, we simulated 4 non-coherent beams propagation through numerical random phase screen and overlapped at the observation plane, and conducted laboratory experiments with phase plates, in the end compared the irradiance fluctuation with individual beam. Both wave optics simulation and laboratory experiments showed the mitigating effect of our model on irradiance fluctuation.

2. Theory analysis

2.1. Non-coherent multi-beam emitting model

In order to obtain non-coherent multi-beam from one laser, firstly, we split one beam into several beams, meanwhile increased the optical path difference (OPD) of each beam, which should be longer than laser coherence length. Then overlapped these beams at the observation plane. Here, we took advantage of the property that with the reduction of laser temporal coherence, the laser spatial coherence reduced. This method could guarantee both the highly coherence of individual beam and lowly coherence of overlapped illumination field.

* Corresponding author.
E-mail address: tianyz@ciomp.ac.cn (Y. Tian).

http://dx.doi.org/10.1016/j.optlastec.2017.06.013
0030-3992/

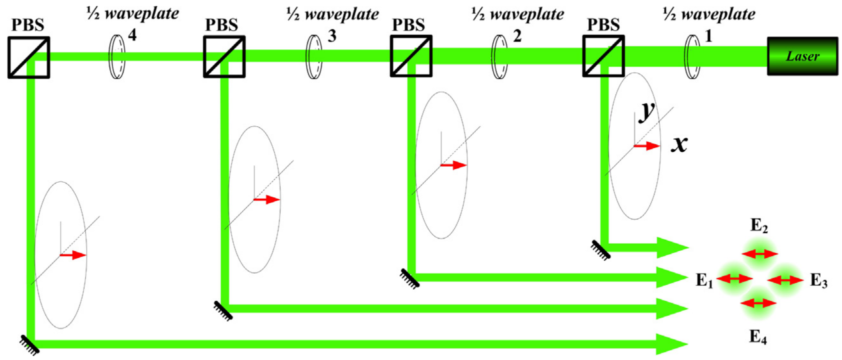

Fig. 1. Non-coherent multi-beam emitting model with changeable intensity of each beam.

According to this idea, we established the non-coherent multi-beam emitting model, as shown in Fig. 1, which 4 beams were generated here. Four groups ½ wave plates, controlling laser polarization angle, and polarization beam splitters (PBS), making sure emitting laser with the same polarization state, were used to split beams and adjust emitting power of each beam. In order to make sure emitting beams were not coherent, 4 beams should divide far enough to ensure the OPD greater than coherent length.

2.2. The mitigating effect on turbulent scintillation of non-coherent multi-beam overlapped illumination

The scintillation index [5], normalized irradiance variation of illumination field, was always used to evaluate the irradiance uniformity and fluctuation when laser propagation through atmosphere, and in this paper we didn't consider the spatial uniformity which could be ignored for laser active imaging and laser communication. If we could deduce the relationship between the scintillation index of single beam and that of non-coherent multi-beam, the mitigating effect on turbulent scintillation of the model, as shown in Fig. 1, could be evaluated. In this section, we studied the relationship of scintillation index only using statistical method but avoided the complexity physical process.

Assuming emitting intensity was I at source, and it split into N non-coherent beams with field U_i, intensity I_i, thus:

$$\langle I\rangle = \sum_{i=1}^{N}\langle I_i\rangle, \tag{1}$$

where $\langle\rangle$ denoted the ensemble average. The irradiance PDF of illumination field of each beam followed lognormal distribution under weak turbulence [5,12]:

$$p_{I_i}(I_i) = \frac{1}{2\sqrt{2\pi\sigma_{\chi_i}^2}I_i}\exp\left\{-\frac{[\ln(I_i/I_0)-2\langle\chi_i\rangle]^2}{8\sigma_{\chi_i}^2}\right\} \quad (I_i \geqslant 0), \tag{2}$$

where $\langle\chi_i\rangle$ and ${\sigma_{\chi i}}^2$ were the mean and variance of lognormal amplitude $\chi = \ln(A/A_0)$ of the i^{th} beam.

Because N beams were non-coherent which meant independent with each other [13] from the point of statistical property, the PDF of N overlapped beams was considered as the PDF of the sum of N independent random variables. Generally, the PDF of the sum of N independent variables was the convolution of their PDFs, or the Fourier transformation of characteristic function (CF) of the sum of variables, was the product of CFs of all these variables. For normal distribution, this operation was easily carried out by their CFs, and the sum distribution was another normal distribution. For lognormal distribution, however, it was known that the CF of log-normal distribution had not been found yet [14]. Fortunately, we could use statistical moments, which could be solved accurately, of the sum distribution to estimate the irradiance fluctuation of multi-beam model.

The sum distribution of N lognormal variables could also be approximated to lognormal model, which was verified using numerical convolution [15], therefore, we could utilize this approximation under appropriate assumption. And the PDF of overlapped multi-beam could be obtained using its moments, which were easy to get, according to the fact that the approximated mean $\langle\chi\rangle$ and variance σ_χ^2 were equal to the first and second moments of the real sum PDF of N independent lognormal variables [15].

Assuming the mean and variance of the amplitude of U_i were $\langle A_i\rangle$ and ${\sigma_{Ai}}^2$, respectively, and the n^{th} moments of A were:

$$\langle A^n\rangle = \int_0^\infty z^n \frac{1}{\sqrt{2\pi}\sigma_\chi^2 z}\exp\left[-\frac{(\ln z-\langle\chi\rangle)^2}{2\sigma_\chi^2}\right]dz. \tag{3}$$

Based on the CF of normal distribution, we could obtain $\langle A^n\rangle$:

$$\begin{aligned}\langle A^n\rangle &= e^{n\langle\chi\rangle}\int_0^\infty e^{it\upsilon}\frac{1}{\sqrt{2\pi}}\exp\left(-\frac{\upsilon^2}{2}\right)d\upsilon \\ &= \exp(n\langle\chi\rangle + \sigma_\chi^2 n^2/2).\end{aligned} \tag{4}$$

Also the n^{th} moments of irradiance I were expressed as:

$$\langle I^n\rangle = \exp(2n\langle\chi\rangle + 2n^2\sigma_\chi^2). \tag{5}$$

Based on Eq. (4) and (5), the 1st and 2nd moments could be obtained:

$$\begin{aligned}&\langle A_i\rangle = e^{\langle\chi_i\rangle+\sigma_{\chi_i}^2/2}; \quad \langle A_i^2\rangle = e^{2\langle\chi_i\rangle+2\sigma_{\chi_i}^2} \\ &\langle I_i\rangle = e^{2\langle\chi_i\rangle+2\sigma_{\chi_i}^2}; \quad \langle I_i^2\rangle = e^{4\langle\chi_i\rangle+8\sigma_{\chi_i}^2}.\end{aligned} \tag{6}$$

The amplitude mean $\langle A\rangle$ and variance ${\sigma_A}^2$ of overlapped field, and the irradiance mean $\langle I\rangle$ and variance D^2 of overlapped field were:

$$\begin{aligned}\langle A\rangle &= \sum_{i=1}^{N}\langle A_i\rangle = \sum_{i=1}^{N}e^{\langle\chi_i\rangle+\sigma_{\chi_i}^2/2}; \\ \sigma_A^2 &= \sum_{i=1}^{N}\sigma_{A_i}^2 = \sum_{i=1}^{N}\langle A_i\rangle^2(e^{\sigma_{\chi_i}^2}-1) \\ \langle I\rangle &= \sum_{i=1}^{N}\langle I_i\rangle = \sum_{i=1}^{N}e^{2\langle\chi_i\rangle+2\sigma_{\chi_i}^2} \\ D^2 &= \sum_{i=1}^{N}D_i^2 = \sum_{i=1}^{N}\langle I_i\rangle^2(e^{4\sigma_{\chi_i}^2}-1),\end{aligned} \tag{7}$$

where ${D_i}^2$ was irradiance variance of the i^{th} beam, it should be noticed that beams were independent with each other, so the cross-terms were eliminated on the right side of Eq. (7). Thus the

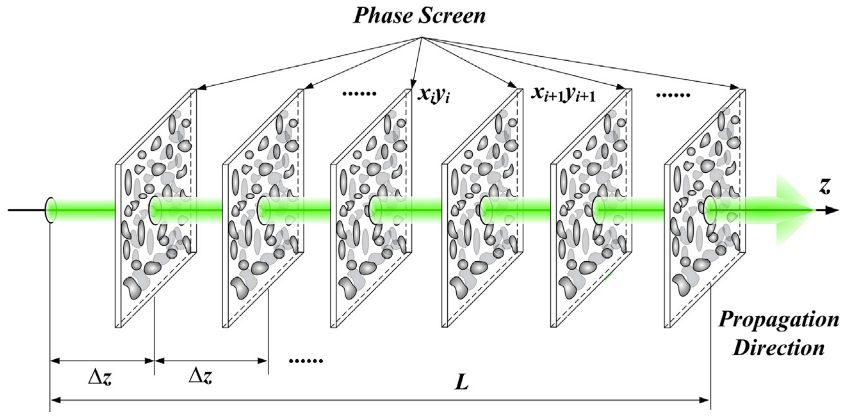

Fig. 2. Simulation model of laser propagation through atmospheric turbulence.

PDF of overlapped field could be approximated as follows, based on Eqs. (2) and (7),

$$p_I(I) = \frac{1}{2\sqrt{2\pi\sigma_\chi^2}I}\exp\left\{-\frac{[\ln(I)-2\langle\chi\rangle]^2}{8\sigma_\chi^2}\right\} \quad (I \geqslant 0), \tag{8}$$

where the lognormal amplitude mean $\langle\chi\rangle$ and variance σ_χ^2 were deduced from Eqs. (6) and (7), and expressed as follows,

$$\begin{aligned}\langle\chi\rangle &= \ln\langle A\rangle - \sigma_\chi^2/2\\ \sigma_\chi^2 &= \ln(\sigma_A^2/\langle A\rangle^2+1).\end{aligned} \tag{9}$$

Now, let's consider the scintillation index of illumination field. For individual beam, it was:

$$\begin{aligned}\sigma_{I_i}^2 &= D_i^2/\langle I_i\rangle^2\\ &= \langle I_i\rangle^2(e^{4\sigma_{\chi_i}^2}-1)/\langle I_i\rangle^2\\ &= e^{4\sigma_{\chi_i}^2}-1.\end{aligned} \tag{10}$$

Eq. (10) showed that the irradiance fluctuation of illumination field was determined only by lognormal amplitude variance σ_χ^2 for individual beam. In the same way, the scintillation index of non-coherent overlapped multi-beam was expressed as:

$$\sigma_I^2 = \frac{D^2}{\langle I\rangle^2} = \frac{\sum_{i=1}^N\langle I_i\rangle^2\sigma_{I_i}^2}{\left(\sum_{i=1}^N\langle I_i\rangle\right)^2}, \tag{11}$$

Eq. (11) showed that the irradiance fluctuation of overlapped field was determined by the mean and variance of irradiance of each beam. It could be proved that only when the mean of irradiance and scintillation index of each single beam equaled to each other,

$$\begin{aligned}&\langle I_1\rangle = \langle I_2\rangle = \cdots = \langle I_i\rangle\cdots = \langle I_N\rangle = \langle I_0\rangle\\ &\sigma_{I_1}^2 = \sigma_{I_2}^2 = \cdots = \sigma_{I_i}^2 = \sigma_{I_N}^2 = \sigma_{I_0}^2\end{aligned} \tag{12}$$

Eq. (11) could obtain minimum,

$$\sigma_{I_{sum}}^2 = \sigma_{I_0}^2/N. \tag{13}$$

Eq. (13) indicated that the scintillation index of overlapped field, $\sigma_{Isum}{}^2$, was reduced to 1/N of the scintillation of individual beam, $\sigma_{Io}{}^2$, when the mean irradiance and scintillation of beams equaled to each other.

Actually, N non-coherent beams always propagated through atmospheric turbulence with the same statistical property for the applications we considered, which meant they shared the same scintillation index [5],

$$\sigma_{I_1}^2 = \sigma_{I_2}^2 = \cdots = \sigma_{I_i}^2 = \sigma_{I_N}^2 = \sigma_{I_0}^2, \tag{14}$$

and that leaded to a general result:

$$\sigma_{I_{sum}}^2 = \frac{D_{sum}^2}{\langle I_{sum}\rangle^2} = \frac{\sigma_{I_0}^2\sum_{i=1}^N\langle I_i\rangle^2}{\langle I_{sum}\rangle^2}. \tag{15}$$

This equation represented the general situation, in which the scintillation index of overlapped illumination field was determined not only by the ratio of single beam irradiance to total irradiance but also scintillation index of single beam.

3. Simulation of non-coherent multi-beam overlapped illumination

Eqs. (11) and (15) described the relationship of scintillation index between multi-beam model and single beam illumination, in this section, we will verify this theory results using numerical wave-optics simulation method.

3.1. Model of propagation through atmosphere for single beam

It was typical that using split-step method and phase screen to simulate laser propagation trough atmosphere, as shown in Fig. 2. The propagation path was divided into N vacuum sections, in the end of which located one phase screen. Laser propagated through these sections one by one, and the phase of optical field was modulated randomly by phase screens to simulate the effect of turbulence. The calculation model was expressed as:

$$\begin{aligned}&U_t(x_{i+1},y_{i+1},z_{i+1})\\ &\quad = \mathbf{F}^{-1}\left\{e^{ikz_i}\exp\left[-i\pi\lambda\Delta z_i(f_{x_i}^2+f_{y_i}^2)\right]\right.\\ &\qquad \left.\times\mathbf{F}[U_t(x_i,y_i,z_i)e^{iS(x_i,y_i,z_i)}]\right\},\end{aligned} \tag{16}$$

where F[$f(x, y)$] was Fourier transform of $f(x, y)$, $\mathbf{F}^{-1}$ was inverse Fourier transform, f_{xi} and f_{yi} were the spatial frequency of x_iy_i plane, Δz_i was the distant from x_iy_i plane to $x_{i+1}y_{i+1}$ plane, and $S(x_i, y_i, z_i)$ was phase modulation introduced by the i^{th} phase screen. In our simulation, we generated FFT phase screens [16] to introduce turbulence influence:

$$S(x,y,z) = \int_0^\infty\int_0^\infty g(\kappa_\perp)\sqrt{0.492r_0^{-5/3}\kappa_\perp^{-11/3}}e^{i\boldsymbol{\kappa}_\perp \mathbf{r}}d\boldsymbol{\kappa}_\perp, \tag{17}$$

where $g(\kappa_\perp)$ was the 2 dimensional (2-D) white noise, $\kappa_\perp$ was the 2-D scale wave number, r_0 was the atmospheric coherent length [3,5] which represented the turbulent situation on the propagation path, and **r** was the vector (x, y, z). Triangular interpolation technology was used to compensate low spatial frequency information [16] of

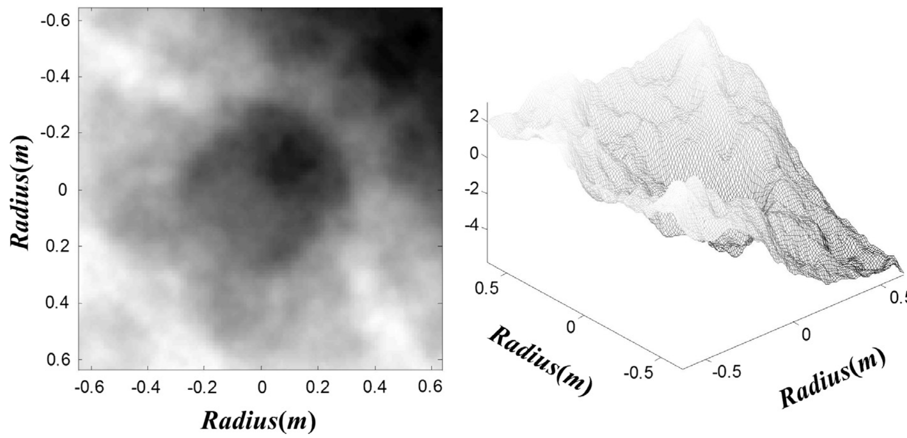

Fig. 3. Phase screen with low frequency compensation.

Table 1
Simulation parameters of turbulence.

L	C_n^2	r_0	L_0	l_0
5.4 km	$\approx 5\times10^{-16}\,\mathrm{m}^{-2/3}$	$\cong$0.05 m	10 m	5 mm

L0 was the outer scale, and l0 was the inner scale.

FFT phase screens, and Fig. 3 was one phase screen with low frequency compensation. Because there were so many papers considered the FFT phase screen method, we would not describe it in detail here.

The atmospheric coherent length r_0 used in Eq. (17) could be expressed as:

$$r_0 = 0.185\left[\frac{\lambda^2}{\int_{z_0}^{z_0+L} C_n^2(\xi)d\xi}\right]^{3/5}, \tag{18}$$

where $C_n{}^2$ was the index-of-refraction structure constant (in units of $m^{-2/3}$), and L was the propagation distance. For split step method, the r_0 should split into r_{0i} [17],

$$r_{0i} = r_0 N_{layer}^{3/5}. \tag{19}$$

Eq. (19) denoted the atmospheric coherent length of each phase screen, and N_{layer} was the number of phase screens used in simulation. Table 1 was the simulation parameters of turbulence used in this paper.

It should be noted that laser was always divergent for the application we discussed in Section 1, therefore, it was better to change the sample interval as the beam diameter increased during propagation, and here we set the calculation model [18,19] as follows,

$$\begin{aligned} &U_t(n_{i+1}, m_{i+1}) \\ &= G_{sg}(n_i, m_i)\exp[ik\Delta z]\exp\left[-i\frac{k(1-\tau_i)}{2\tau_i\Delta z}(n_{i+1}^2 + m_{i+1}^2)\delta_{i+1}^2\right] \\ &\times\mathbf{F}^{-1}\left(\exp\left[-i\frac{\pi\lambda\Delta z}{\tau_i}\left[\left(\frac{n_i}{D_{gridi}}\right)^2 + \left(\frac{m_i}{D_{gridi}}\right)^2\right]\right]\right. \\ &\left.\times\mathbf{F}\left\{\frac{1}{\tau_i}U_t(n_i, m_i)e^{iS(n_i,m_i)}\exp\left[i\frac{k}{2\Delta z}(1-\tau_i)(n_i^2 + m_i^2)\delta_i^2\right]\right\}\right), \\ &\tau_i = \frac{\delta_{i+1}}{\delta_i}, \quad i = 0, 1, \ldots, \frac{L}{\Delta z} - 1 \end{aligned} \tag{20}$$

where $G_{sg}(n, m)$ was the super Gaussian filter function used to control energy overflow,

$$G_{sg}(x, y) = \exp\left[-\left(\frac{\sqrt{x^2+y^2}}{\sigma_{sg}}\right)^{n_{sg}}\right] n_{sg} > 2, \tag{21}$$

δ_i was the sample interval of the i^{th} plane, D_{gridi} was the width of the i^{th} plane, and Δz was the distant between two adjacent plane. The relationship of these parameters were shown in Fig. 4. The relationship between δ_i and Δz could be expressed as:

$$\begin{aligned} &(\delta_n - \delta_0)/2L = (\delta_i - \delta_0)/2L_i \\ &(L_i = \Delta z_0 + \cdots + \Delta z_{i-1}). \end{aligned} \tag{22}$$

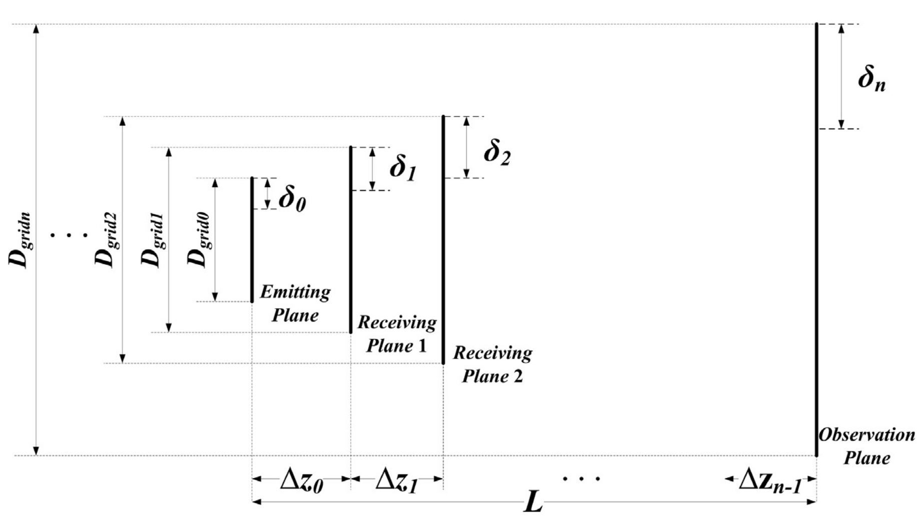

Fig. 4. Sampling parameters.

Table 2
Sampling parameters of phase screens.

N	D_{grid0}	δ_0	D_{gridn}	δ_n	Δz	N_{layer}
1024	0.2131 m	0.2084 mm	9.921 m	9.769 mm	50 m	108

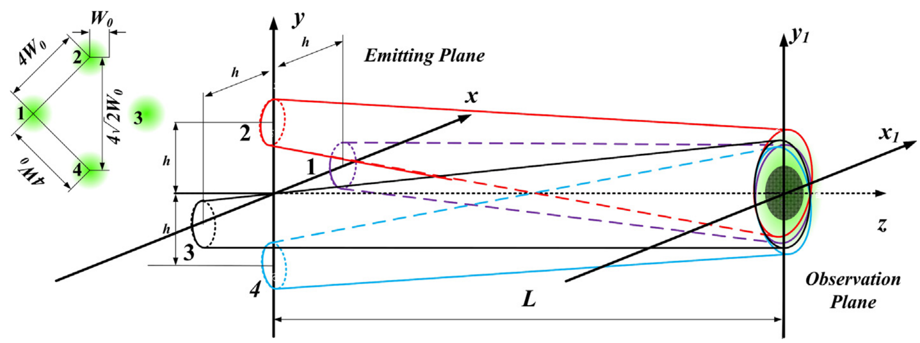

Fig. 5. Simulation model of non-coherent multi-beam overlapped illumination.

Table 3
Laser beam parameters.

λ	W_0	W_1	θ
532 nm	0.02 m	1.98 m	≈0.7 mrad

Table 4
Intensity ratio of each beam to total irradiance.

Group	1	2	3	4	5	6
$a1$	1/10	1/6	1/6	1/8	1/10	1/4
$a2$	1/5	1/6	1/6	1/8	1/10	1/4
$a3$	3/10	1/6	1/3	3/8	1/10	1/4
$a4$	2/5	1/2	1/3	3/8	7/10	1/4
σr	0.3	0.333	0.28	0.3125	0.52	0.25

Table 2 was the sampling parameters of phase screens used here.

3.2. Non-coherent multi-beam overlapped illumination model

The simulation model of non-coherent multi-beam overlapped illumination was shown in Fig. 5, in which 4 beams were generated and propagated through turbulence with the same statistical property, and finally the intensity of beams was overlapped at the observation plane. The position and distance of 4 beams were shown in the left side of Fig. 4. Because each beam was propagation through random phase screens independently and calculated independently, there would be no cross-terms appearing during simulation, which satisfied the assumption that beams should be separated far enough to eliminate scintillation anisoplanatism.

Table 3 was the laser beam parameters used in our simulation, and in the table λ was the wavelength, W_0 was the radius at emitting plane, W_1 was the radius at observation plane, and θ was the divergence angle.

Eq. (15) showed that the ratio of irradiance of each beam to the total intensity played an important role for determining the scintillation index of overlapped field, except scintillation index of single beam illumination, so we chose 6 different groups of the irradiance ratio for simulation, as shown in Table 4. From the first to fourth row, a_i denoted the irradiance ratio, and the last row, σ_r, was the ratio of the scintillation index of overlapped field to that of single beam illumination. The irradiance ratio could be expressed as:

$$\langle I_i \rangle = a_i \langle I_{sum} \rangle \quad \langle I_{sum} \rangle = \sum \langle I_i \rangle. \tag{23}$$

Table 5
Statistical moments of overlapped illumination field (r_0 = 0.05 m, Group 1–6).

Group	$\langle I \rangle$	$\langle \chi \rangle$	$\sigma_\chi{}^2$
1	1.076×10^{-4} W	−0.0359	0.0359
2	1.081×10^{-4} W	−0.0139	0.0139
3	1.081×10^{-4} W	−0.0139	0.0139
4	1.094×10^{-4} W	−0.0128	0.0128
5	1.077×10^{-4} W	−0.0195	0.0195
6	1.079×10^{-4} W	−0.0114	0.0114

Using this equation and Eq. (15), we could obtained σ_r:

$$\sigma^2_{I_{sum}} = \sigma^2_{I_0} \sum_{i=1}^{4} a_i^2 \\ \Rightarrow \\ \sigma_r = \sigma^2_{I_{sum}} / \sigma^2_{I_0} = \sum_{i=1}^{4} a_i^2, \tag{24}$$

For statistical purpose, we recorded 200 frames of the intensity at observation plane, for both individual beam and multi-beam illumination. According to the simulation parameters in Table 2, 108 phase screens were needed (L = 5.4 km, Δz = 50 m) for one frame. Repeat the propagation and illumination processes 200 times, and record these 200 frames of intensity images, for both individual beam and multi-beam. Based on these records, analyze the mitigating effect on turbulent scintillation using non-coherent multi-beam overlapped illumination.

3.3. Simulation results

Compute the mean of irradiance, and the mean and variance of lognormal amplitude of the center data (*radius* = 0) of 200 images of overlapped field, as shown in Table 5. Using these data and Eq. (8), we could obtain the theoretical distributions of the irradiance of overlapped field, and compared them with the results obtained from simulation data, as shown in Fig. 6. It could be found that the simulation data (SD in Fig. 6) fitted theoretical results (TD in Fig. 6) well, which verified that the PDF of the irradiance of multi-beam at observation plane was also lognormal model as assumed in Section 2.

Compute the scintillation index (normalized intensity variation of 200 images) using simulation data, as shown in Table 6. The 2nd row ($\sigma_{Isum}{}^2$) was the scintillation index of multi-beam illumination under 6 groups, the 3rd row ($\sigma_{Isingle}{}^2$) was the scintillation index of single beam illumination, the 4th row σ_r *simulation* was:

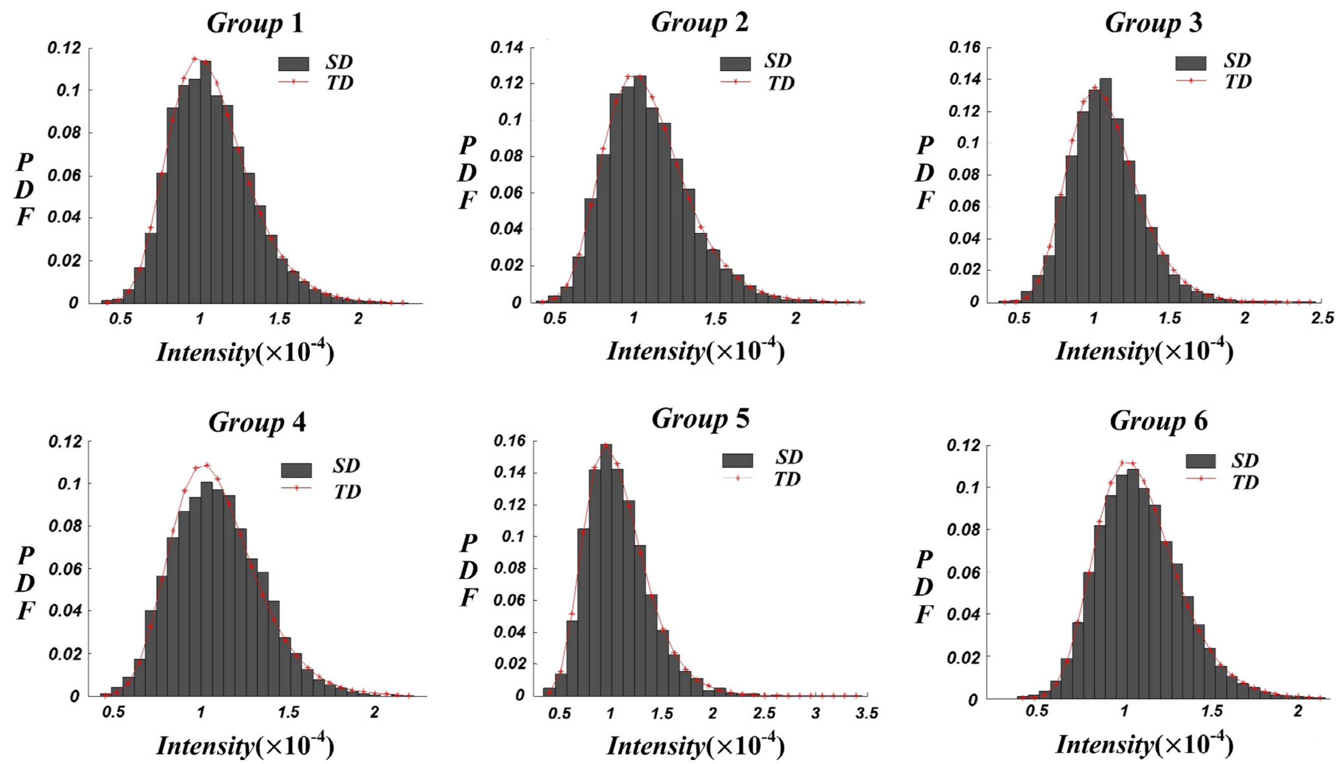

Fig. 6. Irradiance Distribution of Overlapped Field (r_0 = 0.05 m, Group 1–6). (SD was Simulation Data, and TD was Theory Data.)

Table 6
Simulation results of mitigating effect on turbulent scintillation (r_0 = 0.05 m, Group 1–6).

Group	1	2	3	4	5	6
$\sigma_{Isum}{}^2$	0.0483	0.0536	0.0442	0.0502	0.0802	0.0400
$\sigma_{Isingle}{}^2$	0.1509	0.1531	0.1524	0.1521	0.1513	0.1538
σ_r *simulation*	0.32	0.35	0.29	0.33	0.53	0.26
σ_r *theory*	0.3	0.333	0.28	0.3125	0.52	0.25

$$\sigma_r simulation = \sigma^2_{Isum}/\sigma^2_{Isingle},$$

and the 5th row σ_r *theory* represented the reduced ratio of theoretical results, the same as σ_r in Table 4.

Compare the data in Table 4, we could find that non-coherent multi-beam overlapped illumination have mitigating effect on turbulent scintillation, and the simulation results was consistent with the theoretical expectation, which proved the analysis results in Section 2. Especially, the best mitigating effect, which $\sigma_{Isum}{}^2$ reduced to $\sigma_{Isingle}{}^2/4$, was obtained only when the irradiance of 4 beams equaled to each other.

In order to confirm the fact that multi-beam scintillation would be reduced with the beam number N increase when the irradiance of beams was equaled to each other, we compared the results of σ_r *simulation* and σ_r *theory* when using 2, 3, and 4 beams illumination. As shown in Table 7, scintillation of 4 beams illumination was the smallest in all these three situations, therefore, it was clear that the irradiance fluctuation at observation plane reduced with beam number increase.

Table 7
Mitigating effect on turbulent scintillation with 2, 3 and 4 beams.

Beams Num.	2	3	4
a_i	(1/2, 1/2)	(1/3, 1/3, 1/3)	Group 6 in Table 4
$\sigma_{Isum}{}^2$	0.0811	0.0541	0.0400
$\sigma_{Isingle}{}^2$	0.1591	0.1546	0.1538
σ_r *simulation*	0.51	0.35	0.26
σ_r *theory*	1/2	1/3	1/4

4. Experiments of non-coherent multi-beam overlapped illumination

In this section we carried out related experiments to test and verify the results deduced in Sections 2 and 3.

4.1. Experiment system

Establish the non-coherent multi-beam emitting system based on Section 2.1 and Fig. 1, as shown in Fig. 7. The emitting system was composed by laser, beam splitting units, aperture stops, and reflectors. The beam splitting unit was composed by ½ wave plate, PBS, and aperture, as shown in the upper right corner of Fig. 7.

The parameters of the laser we used in experiment were: wavelength 532 nm, power 100 mW, radius at source 0.8 mm,

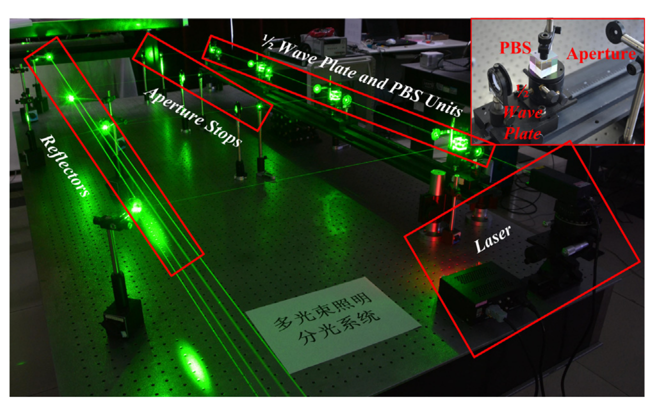

Fig. 7. Non-coherent multi-beam emitting system.

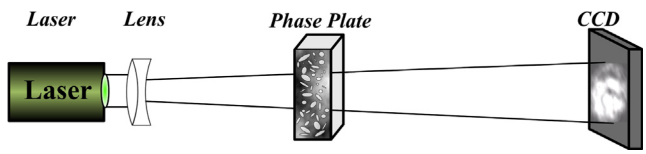

Fig. 8. Experiment setup of Gaussian beam propagation through a random phase screen.

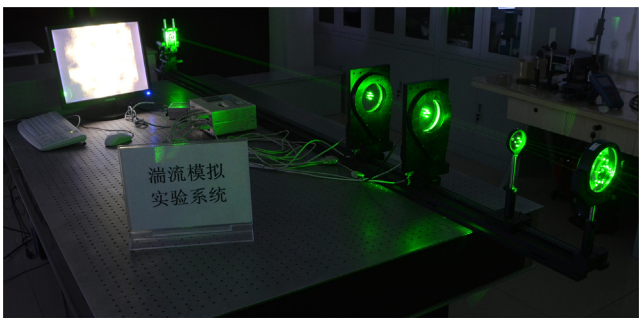

Fig. 9. Turbulent simulation system.

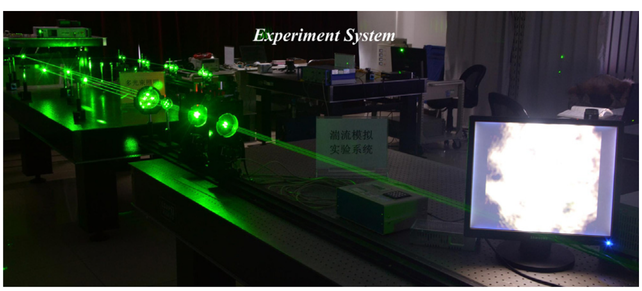

Fig. 10. Non-coherent multi-beam propagation through turbulent simulation system.

divergence angle 3 mramd and coherent length less than 1 m. The OPD of each beam should be longer than laser coherent length in experiment, thus we set the OPD of 4 beams longer than 1.6 m, which was long enough to make sure beams were not coherent with each other, and to eliminate any cross-term between 4 beams.

We used optical lens and thin random phase plate [20], HS-100, a product of Lexitek Inc., with thickness 22 mm and active diameter 83 mm, to set up turbulent simulation system [21,22], as shown in Fig. 8. The emitting laser was transformed by optical lens firstly and propagated through phase plate, finally, the irradiance was recorded by CCD. In order to study the irradiance fluctuation, the CCD camera was used without lens here, and laser illuminated the CCD directly. Some neutral density filters might be used to protect the CCD and make sure it was not saturation. The gray scale images represented the irradiance at observation plane and were recorded.

The model of Gaussian beam propagation through thin phase screen has been given by Andrews et al. [23], and based on their results Tian et al. [24] did some expanding work. According to their work, we could simulate different turbulence situation by moving the phase plate on optical path, and finally establish the experiment system, as shown in Fig. 9. Two phase plates were used, with fixed distant 50 cm, and for single beam propagation, the scintillation index was changed between [0.01, 0.12] using this system by moving the two phase plates. If the readers want more information about this system, please check [23,24] for details.

Combine the non-coherent multi-beam emitting system and the turbulent simulation system, as shown in Fig. 10. Our experiments were conducted based on these two systems.

4.2. Experiment results

In Section 3, 6 groups of different irradiance ratio were used, here we chose 3 groups in Table 4 (Group 1, 5, and 6) to implement the experiments. Three different turbulent situation was considered, and the irradiance at observation plane was recorded using

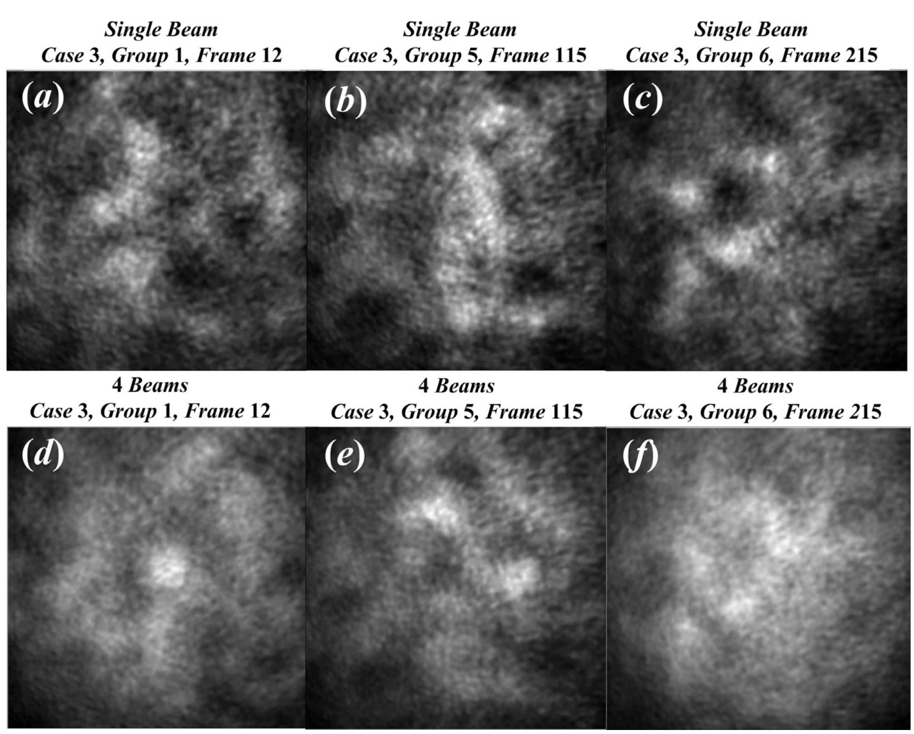

Fig. 11. Illumination field of Single beam ($a \sim c$) and 4 beams ($d \sim f$).

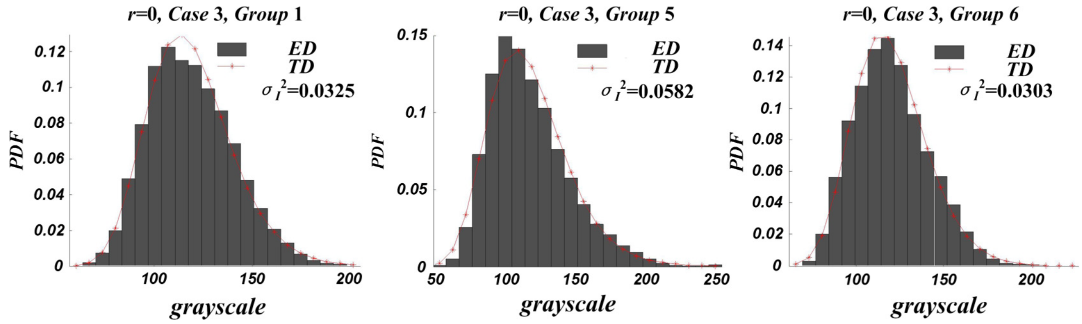

Fig. 12. Irradiance distribution of overlapped illumination field (Group 1, 5, and 6). (ED was Experiment Data, and TD was Theory Data.)

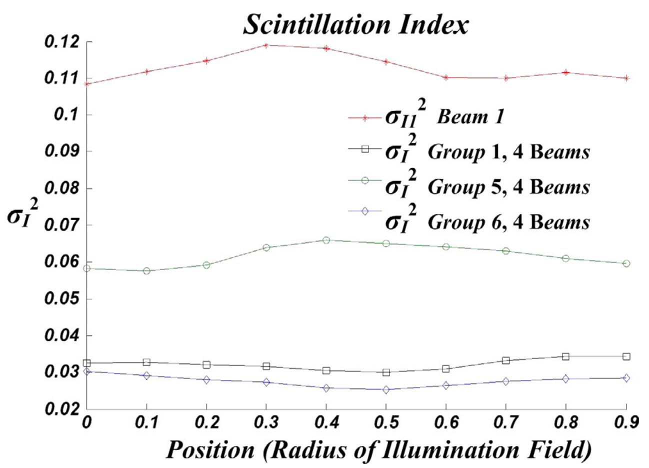

Fig. 13. Illumination field scintillation index of single beam and 4 beams (Group 1, 5, and 6).

Table 8
Comparison of scintillation index between experimental results and theoretical expectation.

Group		Beam 1	Beam 2	Beam 3	Beam 4
1	I_i/I	0.0998	0.1992	0.3005	0.4005
	$\langle\sigma_{Ii}{}^2\rangle$	0.1132	0.1141	0.1141	0.1114
	$\langle\sigma_{Isum}{}^2\rangle$	0.0321			
	$\sigma_{Isum}{}^2$ *theory*	0.0338			
5	I_i/I	0.0994	0.0999	0.1003	0.7005
	$\langle\sigma_{Ii}{}^2\rangle$	0.1183	0.1138	0.1160	0.1146
	$\langle\sigma_{Isum}{}^2\rangle$	0.0617			
	$\sigma_{Isum}{}^2$ *theory*	0.0597			
6	I_i/I	0.2494	0.2489	0.2501	0.2515
	$\langle\sigma_{Ii}{}^2\rangle$	0.1118	0.1193	0.1140	0.1145
	$\langle\sigma_{Isum}{}^2\rangle$	0.0278			
	$\sigma_{Isum}{}^2$ *theory*	0.0287			

grayscale images, for simplification, we took one turbulent situation (case 3 with scintillation index of individual beam ≈0.11) for instance. The same as simulation, 200 images of irradiance for both single beam and multi-beam were recorded.

Fig. 11 was one frame grayscale image of single beam ($a \sim c$) illumination and multi-beam ($d \sim f$). It could be found that the irradiance uniformity of 3 bottom images ($d \sim f$) was better than that of 3 upper images ($a \sim c$), especially the right bottom one (f), which was obtained under group 6 in Table 4.

Fig. 12 was the irradiance histogram of center data (*radius* = 0) of grayscale images (ED in the figure) and the PDF calculated using Eq. (8) (TD in the figure), of which the parameters were obtained from experimental data. It was apparent that the two results were almost consistent, which meant the experiment gave a positive evidence for the theory analysis of our multi-beam model in Section 2, especially for the assumption that the irradiance of overlapped field was also lognormal distribution under weak turbulence.

Fig. 13 was the comparison of scintillation index of single beam (beam 1) and 4 beams illumination under 3 irradiance groups. The data used to calculate scintillation index were sampled from the same radius of illumination field of 200 frames grayscale images, and 10 positions were calculated from center to margin of illumination field at observation plane. The comparison results shown that non-coherent multi-beam overlapped illumination did have mitigating effect on turbulent scintillation, no matter how the irradiance ratio of each beam was, and more uniformity of the ratio was, the more obvious the mitigating effect was.

Table 9
Experimental results of mitigating effect on turbulent scintillation (Group 1, 5, and 6).

	1	5	6
$\langle\sigma_{Isum}{}^2\rangle/\langle\sigma_{Isingle}{}^2\rangle$	0.28	0.53	0.24
σ_r *theory*	0.3	0.52	0.25

Table 8 was the experimental results of scintillation index. The 1st row of each group (I_i/I) was the irradiance ratio of each beam to total irradiance, measured during experiment, the 2nd row of each group ($\langle\sigma_{Ii}{}^2\rangle$) was the mean of scintillation index of single beam, the 3rd row of each group ($\langle\sigma_{Isum}{}^2\rangle$) was the mean of scintillation index of overlapped illumination with 4 beams, and the 4th row of each group ($\sigma_{Isum}{}^2$ *theory*) was the theoretical scintillation index of overlapped illumination calculated by Eq. (11):

$$\sigma^2_{Isum} theory = \sum_{i=1}^{4} \langle I_i/I \rangle^2 \langle \sigma^2_{I_i} \rangle, \tag{25}$$

Table 9 was the experimental results of mitigating effect of our multi-beam model. The 2nd row ($\langle\sigma_{Isum}{}^2\rangle/\langle\sigma_{Isingle}{}^2\rangle$) was the ratio of the scintillation index of overlapped field to that of single beam illumination, and $\langle\sigma_{Isingle}{}^2\rangle$ was the mean of $\langle\sigma_{Ii}{}^2\rangle$ in Table 8. The 3rd row (σ_r *theory*) represented the reduced ratio of theoretical result, the same as σ_r in Table 4.

The results in Tables 8 and 9 showed that: our experiments accorded with the theoretical expectation. For single beam illumination, the turbulent scintillation was determined only by the turbulent situation and had nothing to do with emitting intensity, but for multi-beam illumination, the scintillation index was determined by both the turbulent situation and the irradiance ratio of each beam. Meanwhile, the best mitigating effect on turbulent scintillation could be obtained, $\langle\sigma_{Isum}{}^2\rangle$ reduced to $\langle\sigma_{Isingle}{}^2\rangle/4$, when the observation plane was illuminated by non-coherent multi-beam with equal intensity, and that result was also obtained in Section 3.

Table 10
Mitigating effect on turbulent scintillation with 2, 3 and 4 beams.

Beams Num.	2	3	4
a_i	(1/2, 1/2)	(1/3, 1/3, 1/3)	Group 6 in Table 4
$\langle \sigma_{Isum}{}^2 \rangle$	0.0601	0.0392	0.0278
$\langle \sigma_{Isingle}{}^2 \rangle$	0.1155	0.1152	0.1149
$\langle \sigma_{Isum}{}^2 \rangle / \langle \sigma_{Isingle}{}^2 \rangle$	0.52	0.34	0.26
σ_r *theory*	1/2	1/3	1/4

As the comparison in Table 7, we also compared the experimental results of 2, 3, and 4 beams, as shown in Table 10. It was apparent that when illumination with equal intensity, increasing beam number N could increase the irradiance uniformity at the observation plane, which verified the result of Eq. (13).

5. Conclusions

The mitigating effect on irradiance fluctuation of non-coherent multi-beam illumination model was discussed, under weak turbulence situation. We found a simply way to deduce the relationship between scintillation index of multi-beam illumination and that of single beam, when lognormal model was valid. The multi-beam scintillation index verified that the non-coherent multi-beam illumination model was useful for mitigating the irradiance fluctuation. And we tested our model against wave optics simulation with split-step method and random phase screens, and also laboratory experiments with phase plates. Both the simulation and experiments verified the multi-beam scintillation model, with which the irradiance fluctuation reduced to lowest when the observation plane illuminated by N beams with equal intensity.

Acknowledgments

The authors were very thankful to the reviewers for valuable comments. This work was supported by the Natural Science Foundation of Jilin province under grant NO. 20170520169JH, 20160204069GX.

References

[1] T. Lei, M. Zhang, Y.R. Li, et al., Massive individual orbital angular momentum channels for multiplexing enabled by Dammann gratings, Light Sci. Appl. 4 (2015) 1–7.
[2] X. Yi, Z.J. Liu, P. Yue, Optical scintillations and fade statistics for FSO communications through moderate-to-strong non-Kolmogorov turbulence, Opt. Laser Eng. 47 (2013) 199–207.
[3] D.L. Fried, J.B. Seidman, Laser-beam scintillation in the atmosphere, J. Opt. Soc. Am. 57 (1967) 181–185.
[4] V.I. Tatarskii, Wave Propagation in a Turbulent Medium, McGraw-Hill, 1961.
[5] L.C. Andrews, R.L. Phillips, Laser Beam Propagation through Random Media, 2nd ed., SPIE, 2005.
[6] H. Wang, D.J. Liu, Z.X. Zhou, S.F. Tong, Y.S. Song, Propagation properties of radially polarized partially coherent beam in turbulent atmosphere, Opt. Laser Eng. 49 (2011) 1238–1244.
[7] C.Y. Chen, H.M. Yang, M. Kavehrad, Z. Zhou, Propagation of radial Airy array beams through atmospheric turbulence, Opt. Laser Eng. 52 (2014) 106–114.
[8] Y. Baykal, Field correlations of flat-topped Gaussian and annular beams in turbulence, Opt. Laser Eng. 49 (2011) 647–651.
[9] L.Y. Cui, B.D. Xue, W.F. Xue, X.Z. Bai, X.G. Cao, F.G. Zhou, Expressions of the scintillation index for optical waves propagating through weak non-Kolmogorov turbulence based on the generalized atmospheric spectral model, Opt. Laser Technol. 44 (2012) 2453–2459.
[10] J.A. Tellez, J.D. Schmidt, Multibeam scintillation cumulative distribution function, Opt. Lett. 36 (2011) 286–288.
[11] C. Higgs, H.T. Barclay, K.W. Billman, Multibeam laser illuminator approach, SPIE 3706 (1999) 206–215.
[12] Y.X. Zhang, Z.Y. Chi, Optical Wave Propagation and Imaging through Atmosphere, Bei Jing, 1997.
[13] J.W. Goodman, Speckle Phenomena in Optics: Theory and Application (Q.Z. Cao et al., 2009, Trans.), California, 2007.
[14] J.A. Tellez, J.D. Schmidt, Multiple transmitter performance with appropriate amplitude modulation for free-space optical communication, Appl. Opt. 50 (2011) 4737–4745.
[15] L.F. Fenton, The sum of log-normal probability distributions in scatter transmission systems, Ire Trans. Commun. Syst. 8 (1960) 57–67.
[16] B.J. Herman, L.A. Strugala, Method for inclusion of low-frequency contributions in numerical representation of atmospheric turbulence, SPIE 1221 (1990) 183–192.
[17] T.A. Rhoadarmer, J.R.P. Angel, Low-cost, broadband static phase plate for generating atmospheric like turbulence, Appl. Opt. 40 (2001) 2946–2955.
[18] J.A. Rubio, A. Belmonte, A. Comerón, numerical simulation of long-path spherical wave propagation in three-dimensional random media, J. Opt. Soc. Am. A 38 (1999) 1462–1469.
[19] J.D. Schmidt, Numerical Simulation of Optical Wave Propagation with Examples in Matlab, SPIE, 2005.
[20] Lexitek Inc., Turbulence phase plate, 1997. <http://lexitek.com> (accessed 13.03.2013).
[21] S.V. Mantravadi, T.A. Rhoadarmer, R.S. Glas, Simple laboratory system for generating well-controlled atmospheric-like turbulence, Proc. SPIE 5553 (2004) 290–300.
[22] X.J. Gan, J. Guo, Y.Y. Fu, The simulating turbulence method of laser propagation in the inner field, JPCS 48 (2006) 907–910.
[23] L.C. Andrews, R.L. Phillips, A.R. Weeks, Propagation of a Gaussian-beam wave through a random phase screen, Waves Random Media 7 (1997) 229–244.
[24] Y.Z. Tian, J. Guo, R. Wang, T.F. Wang, Mathematic model analysis of Gaussian beam propagation through an arbitrary thickness random phase screen, Opt. Express 19 (2011) 18216–18228.